Journal of Applied Mathematics and Physics, 2024, 12, 2836-2848
https://www.scirp.org/journal/jamp
ISSN Online: 2327-4379
ISSN Print: 2327-4352

New Lump Solution and Their Interactions with *N*-Solitons for a Shallow Water Wave Equation

Yin Ji, Xiyu Tan*

College of Mathematics and Statistics, Jishou University, Jishou, China
Email: *1326076951@qq.com

How to cite this paper: Ji, Y. and Tan, X.Y. (2024) New Lump Solution and Their Interactions with *N*-Solitons for a Shallow Water Wave Equation. *Journal of Applied Mathematics and Physics*, **12**, 2836-2848.
https://doi.org/10.4236/jamp.2024.128169

Received: July 22, 2024
Accepted: August 13, 2024
Published: August 16, 2024

Abstract

By employing the Hirota's bilinear method and different test functions, the breather solutions of HSI equation with different structures are obtained based on symbolic calculation with perturbation parameters. Some new lump solitons are found in the process of studying the degradation behavior of breather solutions. The interaction between lump solution and soliton solution is constructed in the form of lump solution, and the motion trajectory of lump is obtained. In addition, the theorem of lump solitons and N-solitons superposition is given and proved. The superposition formula of lump is derived from the theorem, and its spatial evolution behavior is given.

Keywords

HSI Equation, Breather-Waves, Lump Solutions, Interaction Solution

1. Introduction

Investigating the soliton solutions of the integrable systems is always an important topic in the soliton theory. Hirota's bilinear method [1] is an effective method to derive soliton solutions of integrable equations. An integrable equation can be converted to bilinear form, we can study from N-soliton solutions [2], Bäcklund transformations [3] [4], Lax pairs and quasi-periodic wave solutions [5]. In recent years, the lump solution in the soliton solution is a special type of soliton solution [6]. A lump solution based on soliton solutions is a rational function solution which is real analytic and decays in all directions of space variables and it can be regarded as one kind of rogue wave [7] [8]. The lump solution not only has important applications in natural sciences, such as optics, quantum field theory and condensed matter physics, but also is used in computer science for data compression and image processing [9] [10]. Breathing waves are also a special type of soliton solution, which undergoes periodic

changes in time [11] [12]. However, when the respiratory wave degenerates into a lump solution, its time variation is eliminated, thus making the form of the solution more simplified [13]. The degeneration process of the respiratory wave and the lump solution involves the mathematical properties of nonlinear partial differential equations and the structure of the solution [11]. Studying this degradation process provides insight into the solutions of the equations and their evolutionary behavior, and reveals the connections and transitions between different types of solutions [14] [15]. The trajectory of lump decomposition in the interaction was also studied [16] [17].

In this paper, we consider a (2 + 1)-dimensional asymmetrical the Hirota-Satsuma-Ito (HSI) shallow water wave equation [18]

$$w_t = u_{xxt} + 3uu_t - 3u_x v_t + \alpha u_x, \ w_x = -u_y, \ v_x = -u. \tag{1}$$

In this paper, the test function is substituted into the HSI equation to obtain its parametric relationship, and then the breather wave solution and kink breather wave solution are obtained after the parametric relationship is brought in. After taking the parameter limit based on the breather wave solution, the new degenerate solution, namely lump type solution is obtained. the degeneracy of breather solution to lump solution, the interaction of positive quadratic function lump solution with soliton solution, lump locus and superposition of higher order lump with N soliton solution are studied. In the first part of the second section, the respiratory wave solution of the equation is obtained based on bilinear form, and the lump shape solution is obtained by parametric limit method. In the second part, the mixed solution is obtained based on the positive quadratic function superposition soliton solution of lump property solution, and the trajectory equation of lump is calculated. In the third section, a theorem of superposition of higher order lump solution and soliton solution is given and proved. Two examples are given and the spatial structure evolution diagram is drawn. Finally, a brief summary is given.

2. Degradation of Breather Solutions and Mixed Lump Solution

2.1. Bilinear Form and Degradation of Breather Solution

Hirota's bilinear method is a powerful technique used to solve integrable systems of partial differential equations. The key idea behind this method is to represent the solutions of the PDE in terms of simple functions that satisfy a bilinear relation.

In the context of finding breather solutions, Hirota's bilinear method offers several advantages compared to other approaches. One of the main differences is that the bilinear form allows for the explicit construction of multisoliton solutions, including breather solutions, in a systematic way. This means that one can directly obtain solutions with a known number of breathers without needing to resort to iterative procedures. Overall, Hirota's bilinear method stands out for its elegance, efficiency, and applicability in capturing the rich dynamics of breather

solutions in integrable systems.

By transformation

$$\begin{cases} u(x,y,t) = u_0 + 2(\ln f)_{xx}, \\ w(x,y,t) = w_0 - 2(\ln f)_{xy}, \\ v(x,y,t) = -u_0 x - 2(\ln f)_x, \end{cases} \tag{2}$$

where f is an unknown function about x, y and t, the Equation (1) becomes the Hirota bilinear form

$$\left(3u_0 D_x D_t + \alpha D_x^2 + D_x^3 D_t + D_t D_y\right) f \cdot f = 0. \tag{3}$$

where the operator $D_{\_}$ is the Hirota's bilinear differential operator defined by [1]. The D-operators are defined by

$$D_x^m D_y^n f \cdot g = \left(\frac{\partial}{\partial x} - \frac{\partial}{\partial x'}\right)^m \left(\frac{\partial}{\partial y} - \frac{\partial}{\partial y'}\right)^n f(x,y,t) g(x',y',t') \Big|_{x=x', y=y'}. \tag{4}$$

The choice of test functions in methods like Hirota's bilinear method, the inverse scattering transform, and other analytical techniques is crucial in determining the structure and properties of soliton and breather solutions. Test functions are often chosen to make the resulting equations more tractable. Exponential functions are frequently used because they simplify differentiation and integration processes. Simple forms such as polynomials, exponentials, or trigonometric functions allow the nonlinear problem to be converted into a more manageable linear or bilinear form. We can also use the inherent symmetry of nonlinear PDEs to provide certain forms for the test functions. For integrable systems, one can use their integrable structure to find specific test functions that make it easier to find soliton and breathing solutions. Similarly, the amplitude of the oscillations in breather solutions can be controlled by the coefficients and exponents in the test functions.

In order to obtain the breather solution, we choose a test function according to the parametric limit method [19]-[21]

$$f(x,y,t) = a_1 \cosh(\tau_1) + a_2 \cos(\tau_2), \tag{5}$$

where $\tau_i = k_i(j_i x + l_i y + s_i t + \gamma_i)$ and $k_i, j_i, l_i, s_i, \gamma_i (i = 1,2)$ are some free real parameters. By substituting (5) into (3) and using the Maple, we can obtain a set of equation constraints as follows

Case 1:

$$\begin{aligned} l_1 &= \frac{j_1\left(j_1^2 k_1^2\left(3a_1^2 j_1^2 k_1^2 - a_1^2 j_2^2 k_2^2 + a_2^2 j_2^2 k_2^2\right) - 3j_2^2 k_2^2\left(a_2^2 j_2^2 k_2^2 + a_1^2 u_0 - a_2^2 u_0\right)\right)}{\left(a_1^2 - a_2^2\right) j_2^2 k_2^2}, \\ s_2 &= 0, \\ l_2 &= \frac{3j_1^2 k_1^2\left(2a_1^2 j_1^2 k_1^2 + a_1^2 j_2^2 k_2^2 + a_2^2 j_2^2 k_2^2\right) + j_1^2 k_1^2\left(a_1^2 - a_2^2\right)\left(j_2^2 k_2^2 - 3u_0\right)}{j_2 k_2\left(a_1^2 - a_2^2\right)}, \\ s_1 &= -\frac{\alpha j_2^2 k_2^2\left(a_1^2 - a_2^2\right)}{3a_1^2 j_1 k_1^2\left(j_1^2 k_1^2 + j_2^2 k_2^2\right)}. \end{aligned} \tag{6}$$

Case 2:

$$j_2 = -\frac{j_1 k_1^2 s_2}{k_2^2 s_2}, l_1 = \frac{j_1\left(3j_1^2 k_1^2 s_1^2 - j_1^2 k_1^2 k_2^2 s_2^2 + \alpha j_1 k_1^2 s_1 - 3k_2^2 s_2^2 u_0\right)}{k_2^2 s_2^2},$$
$$l_2 = \frac{\left(-j_1^2 k_1^2 s_1^2 + 3j_1^2 k_1^2 k_2^2 s_1 s_2^2 + \alpha j_1 k_2^2 s_2^2 + 3k_2^2 s_1 s_2^2 u_0\right) j_1 k_1^2}{k_2^4 s_2^3}. \tag{7}$$

Then, substituting (6) and (5) into (2), we get the breather solutions of (1)

$$\begin{cases} u(x,y,t) = u_0 + \dfrac{2\left(a_1 k_1^2 j_1^2 \cosh(\tau_1) - a_2 k_2^2 j_2^2 \cos(\tau_2)\right)}{a_1 \cosh(\tau_1) + a_1 \cos(\tau_2)} \\ \quad - \dfrac{2\left(a_1 k_1 j_1 \sinh(\tau_1) - a_2 k_2 j_2 \sin(\tau_2)\right)^2}{\left(a_1 \cosh(\tau_1) + a_1 \cos(\tau_1)\right)^2}, \\ w(x,y,t) = w_0 - \dfrac{2\left(\dfrac{a_1 k_1^2 j_1^2 \rho_1 \cosh(\tau_1)}{\left(a_1^2 - a_2^2\right) j_2^2 k_2^2} - \dfrac{a_2 \rho_2 \cos(\tau_2)}{a_1^2 - a_2^2}\right)}{a_1 \cosh(\tau_1) + a_2 \cos(\tau_2)} \\ \quad + \dfrac{2\left(a_1 k_1 j_1 \sinh(\tau_1) - a_2 k_2 j_2 \sin(\tau_2)\right)\left(\dfrac{a_1 k_1^2 j_1^2 \rho_1 \sinh(\tau_1)}{\left(a_1^2 - a_2^2\right) j_2^2 k_2^2} - \dfrac{a_2 \rho_2 \sin(\tau_2)}{k_2 j_2 \left(a_1^2 - a_2^2\right)}\right)}{\left(a_1 \cosh(\tau_1) + a_2 \cos(\tau_2)\right)^2}, \\ v(x,y,t) = -u_0 x - \dfrac{2\left(a_1 k_1 j_1 \sinh(\tau_1) - a_2 k_2 j_2 \sin(\tau_2)\right)}{a_1 \cosh(\tau_1) + a_2 \cos(\tau_2)}, \end{cases} \tag{8}$$

with

$$\tau_1 = k_1 j_1 x + k_1 \frac{j_1\left(j_1^2 k_1^2\left(3a_1^2 j_1^2 k_1^2 - a_1^2 j_2^2 k_2^2 + a_2^2 j_2^2 k_2^2\right) - 3j_2^2 k_2^2\left(a_2^2 j_2^2 k_2^2 + a_1^2 u_0 - a_2^2 u_0\right)\right) y}{\left(a_1^2 - a_2^2\right) j_2^2 k_2^2}$$
$$- k_1 \frac{\alpha j_2^2 k_2^2\left(a_1^2 - a_2^2\right) t}{3a_1^2 j_1 k_1^2\left(j_1^2 k_1^2 + j_2^2 k_2^2\right)} + k_1 \gamma_1,$$
$$\tau_2 = k_2\left(j_2 x + \frac{3j_1^2 k_1^2\left(2a_1^2 j_1^2 k_1^2 + a_1^2 j_2^2 k_2^2 + a_2^2 j_2^2 k_2^2\right) + j_1^2 k_1^2\left(a_1^2 - a_2^2\right)\left(j_2^2 k_2^2 - 3u_0\right) y}{j_2 k_2\left(a_1^2 - a_2^2\right)} + \gamma_2\right), \tag{9}$$
$$\rho_1 = 3a_1^2 j_1^4 k_1^4 - 3a_2^2 j_2^4 k_2^4 - j_2^2 k_2^2\left(a_1^2 - a_2^2\right)\left(j_1^2 k_1^2 + 3u_0\right),$$
$$\rho_2 = 3j_1^2 k_1^2\left(2a_1^2 j_1^2 k_1^2 + j_2^2 k_2^2\left(a_1^2 + a_2^2\right)\right) + j_2^2 k_2^2\left(a_1^2 - a_2^2\right)\left(j_2^2 k_2^2 - 3u_0^2\right).$$

Perturbation parameters play a crucial role in the symbolic calculation of solutions in nonlinear PDEs. These parameters help to systematically construct solutions by expanding them in a series, facilitating the handling of nonlinearities. Perturbation parameters can be tuned to match specific boundary conditions or physical constraints, ensuring the resulting solutions are physically meaningful. If we take a special choice for the parameters:

$$\gamma_3 = \gamma_2 = \gamma_1 = 0, a_1 = -\frac{6}{5}, a_2 = 1, k_1 = \frac{1}{4}, k_2 = \frac{1}{2},$$
$$j_1 = \frac{3}{2}, j_2 = -\frac{1}{2}, u_0 = w_0 = 1, \alpha = \frac{1}{2}, \tag{10}$$

the breather solution will be obtained, as shown in Figure 1.

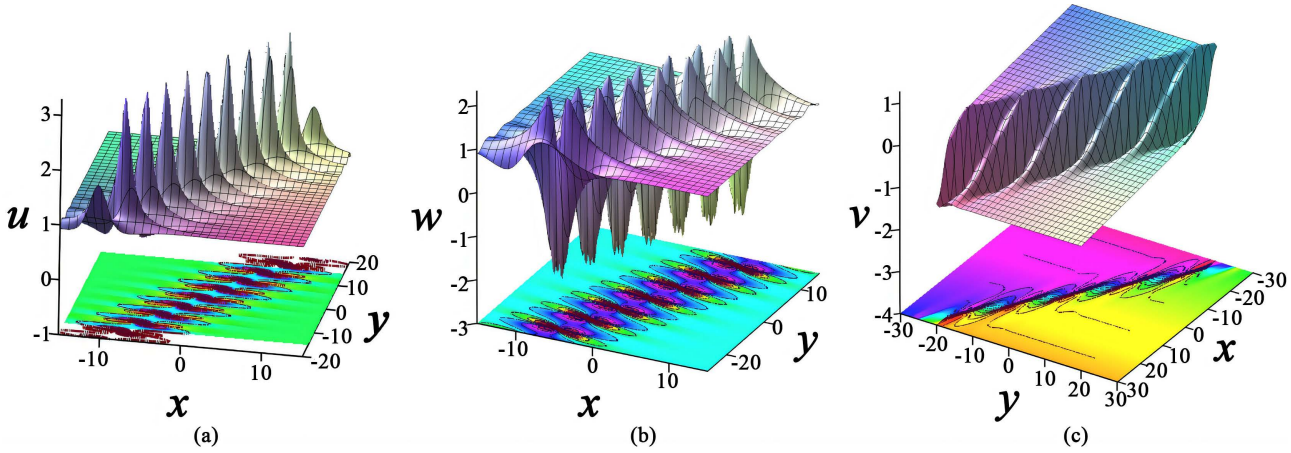

Figure 1. The space structure of breather solution (8) as $t=0$.

Based on the parameter limit method, we further study the degradation behavior of breather solution. We can take the parametric relationship as $k_2 = rk_1$, $a_1 = \beta\cosh(k_1)$, $a_2 = -\beta\cos(k_1)$ in (8), letting the parameter k_1 to approach zero in (8), we get

$$f = \frac{\beta\theta_1^2}{72} + \frac{\beta r^2\theta_2^2}{2} + \beta, \tag{11}$$

with

$$\begin{aligned}\theta_1 &= \frac{-6r^2 j_1^2 j_2^2\left(r^2 j_2^2 + j_1^2\right)x + 9j_1^2\left(r^2 j_2^2 + j_1^2\right)\left(r^4 j_2^4 + 2r^2 j_2^2 u_0 - j_1^4\right)y + 4\alpha r^4 j_2^4 t - 6\gamma_1 r^2 j_1 j_2^2\left(r^2 j_2^2 + j_1^2\right)}{j_1\left(r^2 j_2^2 + j_1^2\right)j_2^2 r^2} \\ \theta_2 &= j_2 x + \frac{1}{2}\frac{\left(6\beta^2 r^2 j_1^2 j_2^2 - 6\beta^2 r^2 j_2^2 u_0 + 6\beta^2 j_1^4\right)y}{j_2\beta^2 r^2} + \gamma_2.\end{aligned} \tag{12}$$

Substituting (11) and (12) into (2), we have

$$u(x,y,t) = u_0 + \frac{2\left(\frac{\beta\left(-6r^4 j_1^2 j_2^4 - 6r^2 j_1^4 j_2^2\right)^2}{36j_1^2\left(r^2 j_2^2 + j_1^2\right)^2 J_2^4 r^4} + \beta r^2 j_2^2\right)}{\frac{\beta(\theta_1)^2}{72} + \beta + \frac{\beta r^2(\theta_2)^2}{2}} - \frac{2\left(\frac{\beta(\theta_1)\left(-6r^4 j_1^2 j_2^4 - 6r^2 j_1^4 j_2^2\right)}{36j_1\left(r^2 j_2^2 + j_1^2\right)J_2^2 r^2} + \beta r^2(\theta_2) j_2\right)^2}{\left(\frac{\beta(\theta_1)^2}{72} + \beta + \frac{\beta r^2(\theta_2)^2}{2}\right)^2},$$

$$w(x,y,t) = w_0 - \frac{2\left(\frac{\beta\left(r^4 j_2^4 + 2r^2 j_2^2 u_0 - J_1^4\right)\left(-6r^4 j_1^2 j_2^4 - 6r^2 j_1^4 j_2^2\right)}{4\left(r^2 j_2^2 + j_1^2\right)j_2^4 r^4} + \frac{6\beta^2 r^2 j_1^2 j_2^2 - 6\beta^2 r^2 j_2^2 u_0 + 6\beta^2 j_1^4}{2\beta}\right)}{\frac{\beta(\theta_1)^2}{72} + \beta + \frac{\beta r^2(\theta_2)^2}{2}}$$

$$+ \frac{2\left(\frac{\beta\theta_1\left(-6r^4 j_1^4 j_2^4 - 6r^2 j_1^4 j_2^2\right)}{36j_1\left(r^2 j_2^2 + j_1^2\right)j_2^2 r^2} + \beta r^2\theta_2 j_2\right)\left(\frac{\beta\theta_1\left(r^4 j_2^4 + 2r^2 j_2^2 u_0 - j_1^4\right)}{4j_2^2 r^2} + \frac{\theta_2\left(6\beta^2 r^2 j_1^2 J_2^2 - 6\beta^2 r^2 j_2^2 u_0 + 6\beta^2 J_1^4\right)}{2\beta j_2}\right)}{\left(\frac{\beta(\theta_1)^2}{72} + \beta + \frac{\beta r^2(\theta_1)^2}{2}\right)^2},$$

$$v(x,y,t)=u_0x-\frac{2\left(\frac{\beta(\theta_1)\left(-6r^4j_1^2j_2^4-6r^2j_1^4j_2^2\right)}{36j_1\left(r^2j_2^2+j_1^2\right)j_2^2r^2}+\beta r^2(\theta_2)j_2\right)}{\frac{\beta(\theta_1)^2}{72}+\beta+\frac{\beta r^2(\theta_2)^2}{2}},\tag{13}$$

the lump solution will be obtained, as shown in Figure 2.

Lump solitons are characterized by their localization in both spatial dimensions. This means that the amplitude of the solution decays rapidly to zero as one moves away from the center of the soliton in any direction. Lump solitons have a characteristic velocity and shape that are preserved during propagation. The velocity can be determined from the parameters of the polynomial function. The shape is typically analyzed by plotting the solution at different time instances to confirm that it remains unchanged. Lump solitons can exhibit elastic collisions, where they pass through each other and emerge with the same shape and velocity.

It can be clearly seen from Figure 1 that u and w are periodic breather wave solutions, and v is manifested as a kinky type breather wave solution, and w appears as the opposite form of v. When k_1 in the test function approaches zero, the trigonometric hyperbolic functions become a positive quadratic function, and the solution of periodic breather characteristics becomes a single lump solution as shown in Figure 2, where u has one peak and two valleys, w is just the opposite of u, and v has one peak and one valley. We noticed that the lump solution u has an upward peak and two downward valleys, and the lump structure with this form is called bright lump structure.

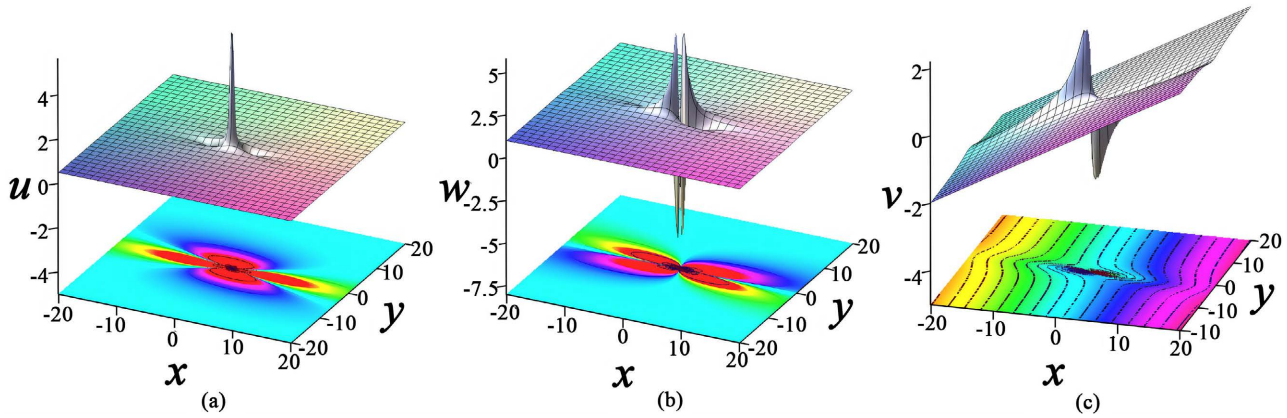

Figure 2. The space structure of lump-type solution (13) as $t=0$.

2.2. The Mixed Lump Solution

In the form of Equations (11) and (12), we consider positive quadratic solutions of (1), the largest class of quadratic functions can be expressed as

$$f=p^2+q^2+c_9,\tag{14}$$

with

$$\begin{aligned} p &= c_1 x + c_2 y + c_3 t + c_4, \\ q &= c_5 x + c_6 y + c_7 t + c_8. \end{aligned} \tag{15}$$

To get the mixed lump stripe solutions of (1), we take

$$f = p^2 + q^2 + c_9 + \mathrm{e}^{j_1 x + l_1 y + s_1 t}, \tag{16}$$

where j_1, l_1, s_1 and $c_i, (1 \le i \le 9)$ are real parameters to be determined. Substituting (16) into (3) and collecting all the coefficients about x, y, t and $\mathrm{e}^{j_1 x + l_1 y + s_1 t}$ and using the Maple, we can obtain a set of equation constraints as follows

Case 1:

$$\begin{aligned} &c_1 = \frac{3c_7 j_1^2}{2\alpha}, c_2 = -\frac{3j_1^2(\alpha c_5 + 3c_7 u_0)}{2\alpha}, c_3 = -\frac{2\alpha c_5}{3j_1^2}, \\ &c_6 = -\frac{3\left(-3c_7^4 j_1^4 + 4\alpha c_5 u_0\right)}{4\alpha}, c_9 = 0, l_1 = \frac{j_1\left(j_1^2 - 6u_0\right)}{2}, s_1 = -\frac{2\alpha}{3j_1}. \end{aligned} \tag{17}$$

Case 2:

$$\begin{aligned} &c_1 = -\frac{3c_7 j_1^2}{2\alpha}, c_2 = \frac{3c_5 j_1^2}{2}, c_3 = \frac{2\alpha c_5}{3j_1^2}, \\ &c_6 = \frac{9c_7 j_1^4}{4\alpha}, c_9 = 0, l_1 = \frac{j_1^3}{2}, s_1 = -\frac{2\alpha}{3j_1}, u_0 = 0. \end{aligned} \tag{18}$$

Then, by substituting (17) into (16), we get

$$\begin{aligned} p &= \frac{3c_7 j_1^2 x}{2\alpha} - \frac{3j_1^2(\alpha c_5 + 3c_7 u_0)y}{2\alpha} - \frac{2\alpha c_5 t}{3j_1^2} + c_4, \\ q &= c_5 x - \frac{3\left(-3c_7 j_1^4 + 4\alpha c_5 u_0\right)y}{4\alpha} + c_7 t + c_8, \end{aligned} \tag{19}$$

and we obtain a 1-lump-1-soliton solution

$$\begin{aligned} u = u_0 &+ \frac{2\left(\frac{9c_7^2 j_1^4}{2\alpha^2} + 2c_5^2 + j_1^2 \mathrm{e}^{-\frac{2\alpha t}{3j_1} + j_1 x + \frac{j_1\left(j_1^2 - 6u_0\right)}{2} y}\right)}{p^2 + q^2 + \mathrm{e}^{j_1 x + \frac{j_1\left(j_1^2 - 6u_0\right)y}{2} - \frac{2\alpha t}{3j_1^2}}} \\ &- \frac{2\left(\frac{3pc_7 j_1^2}{\alpha} + 2qc_5 + j_1 \mathrm{e}^{-\frac{2\alpha t}{3j_1^2} + j_1 x + \frac{rj_1\left(j_1^2 - 6u_0\right)}{2}}\right)^2}{p^2 + q^2 + \mathrm{e}^{j_1 x + \frac{j_1\left(j_1^2 - 6u_0\right)y}{2} - \frac{2\alpha t}{3j_1^2}}}. \end{aligned} \tag{20}$$

In the following, we consider the properties of the lump solution. By substituting (16) into (3), the extreme value theorem gives x and y peaks

$$x = \frac{(c_2 c_7 - c_3 c_6)t + c_2 c_8 - c_4 c_6}{c_1 c_6 - c_2 c_5}, y = -\frac{(c_1 c_7 - c_3 c_5)t + c_1 c_8 - c_4 c_5}{c_1 c_6 - c_2 c_5}. \tag{21}$$

Substituting (17) into (21), in the (x, y) plane, the trajectory equation of lump is

$$y=\frac{\frac{3c_7^2j_1^2}{2\alpha}+\frac{2\alpha c_5^2}{3j_1^2}}{\frac{3j_1^2\left(\alpha c_5+3c_7u_0\right)c_7}{2\alpha}+\frac{c_5\left(-3c_7j_1^4+4\alpha c_5u_0\right)}{2j_1^2}}x+\frac{\frac{2\alpha c_5c_8}{3j_1^2}+c_4c_7}{\frac{3j_1^2\left(\alpha c_5+3c_7u_0\right)c_7}{2\alpha}+\frac{c_5\left(-3c_7j_1^4+4\alpha c_5u_0\right)}{2j_1^2}}. \tag{22}$$

We take a special choice for the parameters:

$$c_4=-\frac{4}{5},c_5=-\frac{3}{2},c_7=-\frac{1}{5},c_8=\frac{3}{4},j_1=-\frac{4}{2},u_0=1,\alpha=\frac{1}{2}, \tag{23}$$

the 1-lump-1-soliton solution will be obtained, as shown in Figure 3.

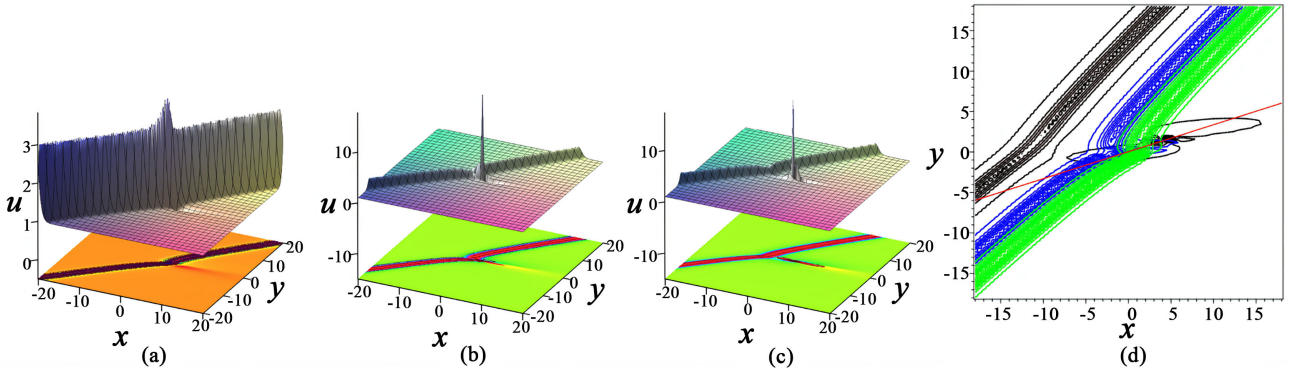

Figure 3. The spatial structure of 1-lump-1-soliton solution (20): (a) $t=30$; (b) $t=0$; (c) $t=-30$; (d) The trajectory of the lump $y=\frac{1}{3}x+\frac{53}{1602}$ (red), when $t=30$ (green), 0 (blue), −30 (black).

Figure 3 clearly demonstrates the collision process of the 3-dimensional spatial structure of lump solution and soliton solution. It can be seen from the Equation (20) that the coefficient before the soliton solution t is $-\frac{2\alpha}{3j_1}$, α and j_1 are both positive values in the parameters. When t in the positive quadratic function tends to positive infinity, the lump solution is slowly absorbed by the collision of soliton solution, while when t tends to negative infinity, lump solution and soliton solution exist simultaneously and lump solution moves in the $y=\frac{1}{3}x+\frac{53}{1602}$ direction.

3. Interaction and Trajectories of Lump Solution and N-Solitons

When $a=0$, the Equation (3) becomes

$$\left(D_x^3D_t+D_yD_t+3u_0D_xD_t\right)f\cdot f=0, \tag{24}$$

then we study the interaction of lump and N-soliton solutions and the motion trajectory of lump solutions. the following form of function is selected

$$\begin{aligned} &f(x,y,t)=\Phi(x,y,t)+\Psi(x,y,t),\\ &\Phi(x,y,t)=b_0+\sum_{i=1}^{M}\left(m_i x+n_i y+b_i t+d_i\right)^2,\\ &\Psi(x,y,t)=\sum_{j=1}^{N}a_j \mathrm{e}^{k_j x+l_j y+s_j t+\gamma_j}, \end{aligned} \tag{25}$$

where $b_0, m_i, n_i, b_i, d_i\,(i=1,2,\cdots,M)$ and $a_j, k_j, l_j, s_j, \gamma_j\,(j=1,2,\cdots,N)$ are free real parameters. For $i=2$, $\Phi(x,y,t)$ is a first-order lump solution, for $j=1$, $\Psi(x,y,t)$ is in the form of a first-order soliton solution, the function $f(x,y,t)$ consists of lump solution form and soliton solution form. By substituting (25) into Equation (24), we can study the new spatial structure and dynamic behavior of Equation (1).

Theorem. If $s_j=0$, $n_i=-3u_0m_i$, $l_j=-k_j^3-3u_0k_j$, $\sum_{i=1}^{M}m_ib_i=0$ and $\Phi(x,y,t)$ is a solution of (24), then $f(x,y,t)$ is a solution of (24).

Proof. Substituting (25) into (24), and we want to prove

$$\begin{aligned} &\left(D_x^3D_t+D_yD_t+3u_0D_xD_t\right)f\cdot f\\ &=\left(\left(D_x^3+D_y+3u_0D_x\right)D_t\right)\left(\Phi\cdot\Phi+\Phi\cdot\Psi+\Psi\cdot\Phi+\Psi\cdot\Psi\right)=0, \end{aligned} \tag{26}$$

$\Phi(x,y,t)$ is a solution to the equation, and $s_j=0$, then

$$\left(\left(D_x^3+D_y+3u_0D_x\right)D_t\right)(\Phi\cdot\Phi)=0,\left(\left(D_x^3+D_y+3u_0D_x\right)D_t\right)(\Psi\cdot\Psi)=0, \tag{27}$$

therefore

$$\begin{aligned} &\left(\left(D_x^3+D_y+3u_0D_x\right)D_t\right)(f\cdot f)\\ &=2\left(\left(D_x^3+D_y+3u_0D_x\right)D_t\right)(\Phi\cdot\Psi)\\ &=2\left(D_x^3+D_y+3u_0D_x\right)\left(\Phi_t\Psi-\Phi\Psi_t\right)\\ &=2\left(\Phi_{txxx}\Psi-3\Phi_{txx}\Psi_x+3\Phi_{tx}\Psi_{xx}-\Phi_t\Psi_{xxx}\right)\\ &\quad+2\left(\Phi_{ty}\Psi-\Phi_t\Psi_y\right)+6u_0\left(\Phi_{tx}\Psi-\Phi_t\Psi_x\right)\\ &=2\left(\left(\Phi_{ty}+3u_0\Phi_{tx}\right)\Psi-\Phi_t\left(\Psi_y+\Psi_{xxx}+3u_0\Psi_x\right)+3\Phi_{tx}\Psi_{xx}\right). \end{aligned} \tag{28}$$

According to (25), we get

$$\begin{aligned} &\Phi_{ty}+3u_0\Phi_{tx}=\sum_{i=1}^{M}2b_i\left(n_i+3u_0m_i\right)=0,\\ &\Psi_y+\Psi_{xxx}+3u_0\Psi_x=\sum_{j=1}^{N}\left(a_jl_j+a_jk_j^3+3u_0a_jk_j\right)\mathrm{e}^{\tau_j}=0,\\ &\Phi_{tx}\Psi_{xx}=\sum_{i=1}^{M}m_ib_i\sum_{j=1}^{N}a_jk_j^2\mathrm{e}^{\tau_j}=0. \end{aligned} \tag{29}$$

Substituting (29) into (28), the proof is finished.

When $M=2, N=0$, substituting $\Phi(x,y,t)$ into (3) with the aid of symbolic computation, we can obtain a set of equation constraints as follows

$$m_1=-\frac{b_2m_2}{b_1}, n_1=-3u_0m_1, n_2=-3u_0m_2. \tag{30}$$

By substituting (30) into function $\Phi(x,y,t)$, we have

$$\Phi(x,y,t)=b_0+\left(-\frac{b_2m_2}{b_1}x-3u_0m_1y+b_1t+d_1\right)^2+\left(m_2x-3u_0m_2y+b_2t+d_2\right)^2. \tag{31}$$

Further, substituting (31) and (25) into (2), we get the 1-lump-N-soliton solutions of (1)

$$u = u_0 + 2\left(\frac{2m_1^2 + 2m_2^2 + \sum_{j=1}^{N} a_j k_j^2 \mathrm{e}^{\delta_n}}{b_0 + \theta_1^2 + \theta_2^2 + \sum_{j=1}^{N} a_j \mathrm{e}^{\delta_n}} - \frac{\left(2m_1\theta_1 + 2m_2\theta_2 + \sum_{j=1}^{N} a_j k_j \mathrm{e}^{\delta_n}\right)^2}{\left(b_0 + \theta_1^2 + \theta_2^2 + \sum_{j=1}^{N} a_j \mathrm{e}^{\delta_n}\right)^2}\right), \quad (32)$$

with

$$\begin{aligned} \theta_1 &= -\frac{b_2 m_2}{b_1} x - 3u_0 m_1 y + b_1 t + d_1, \\ \theta_2 &= m_2 x - 3u_0 m_2 y + b_2 t + d_2, \\ \delta_n &= k_n x - \left(k_n^3 + 3u_0 k_j\right) y + r_n. \end{aligned} \quad (33)$$

In the following, we consider the properties of the lump solution. by substituting (31) into (24), the extreme value theorem gives x and y peaks

$$x = -\frac{b_1 n_2 t - b_2 n_1 t + d_1 n_2 - d_2 n_1}{m_1 n_2 - m_2 n_1}, y = \frac{b_1 m_2 t - b_2 m_1 t + d_1 m_2 - d_2 m_1}{m_1 n_2 - m_2 n_1}. \quad (34)$$

Substituting (30) into (34), in the (x, y) plane, the trajectory equation of lump is

$$y = -\frac{b_1 m_2 + \frac{b_2^2 m_2}{b_1}}{-3b_1 m_2 u_0 + 3b_2 m_1 u_0} x - \frac{b_1 d_2 - b_2 d_1}{-3b_1 m_2 u_0 + 3b_2 m_1 u_0}. \quad (35)$$

When $N = 1$, we make a special choice for the parameters:

$$\begin{aligned} &m_1 = \frac{3}{2}, m_2 = \frac{2}{5}, a_1 = \frac{4}{5}, b_0 = u_0 = 1, b_1 = \frac{1}{5}, b_2 = \frac{1}{4}, \\ &d_1 = 1, d_2 = -\frac{1}{2}, r_1 = 0, k_1 = \alpha = \frac{1}{2}, \end{aligned} \quad (36)$$

we obtain the following mixed lump stripe solution to (1), as shown in Figure 4.

Figure 4 demonstrates the collision process of three-dimensional spatial structure of lump mixed solution. It can be seen from Equation (32) that the coefficient before the soliton solution t is 0, Therefore, when t in the positive quadratic function tends to positive infinity, 1-lump solution and soliton solution exist simultaneously and lump solution moves along the direction $y = -\frac{41}{177}x + \frac{70}{177}$; while when t tends to negative infinity, lump solution is slowly absorbed after collision by soliton solution.

When $N = 2$, we make a special choice for the parameters

$$\begin{aligned} &m_1 = \frac{3}{2}, m_2 = \frac{2}{5}, a_1 = \frac{4}{5}, b_0 = 1, b_1 = \frac{1}{5}, b_2 = \frac{1}{4}, \alpha = \frac{1}{2}, \\ &k_1 = a_2 = \frac{1}{2}, d_1 = 1, d_2 = k_2 = -\frac{1}{2}, u_0 = 1, r_1 = r_2 = 0, \end{aligned} \quad (37)$$

The spatial structure and evolutionary behavior of the 1-lump-2-soliton solution are shown in Figure 5.

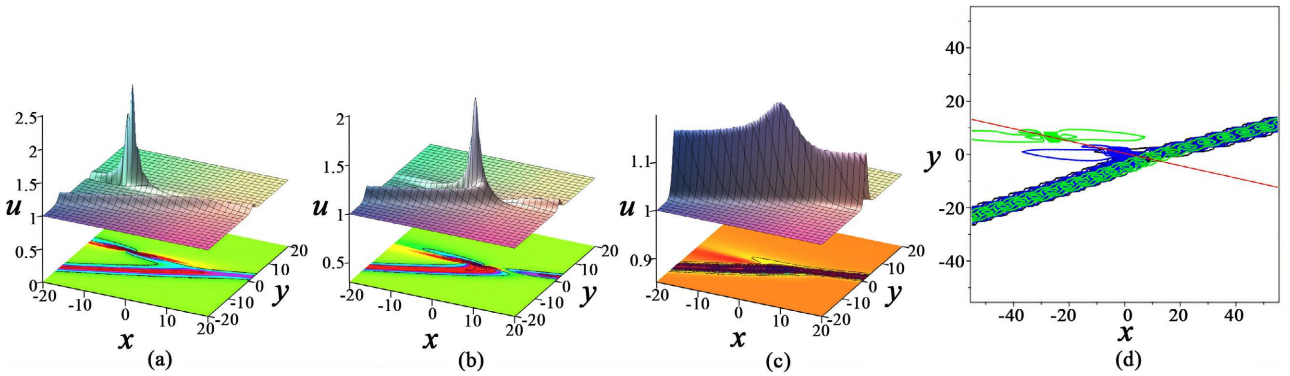

Figure 4. The spatial structure of 1-lump-N-soliton solution at $N = 1$: (a) $t = 30$; (b) $t = 0$; (c) $t = -30$; (d) The trajectory of the lump $y = -\frac{41}{177}x + \frac{70}{177}$ (red), when $t = 30$ (green), 0 (blue), −30 (black).

Figure 5 shows the spatial structure changes of lump mixed solution with time. It can be seen from Equation (32) that the coefficient before the soliton solution t is 0, so when $t = 0$ in the positive quadratic function, lump exists between the two solitons and moves towards lump in the direction $y = -\frac{41}{177}x + \frac{70}{177}$. When t approaches positive infinity, lump is slowly absorbed by the soliton solution collision, and when t approaches negative infinity, lump is slowly absorbed by another soliton solution collision.

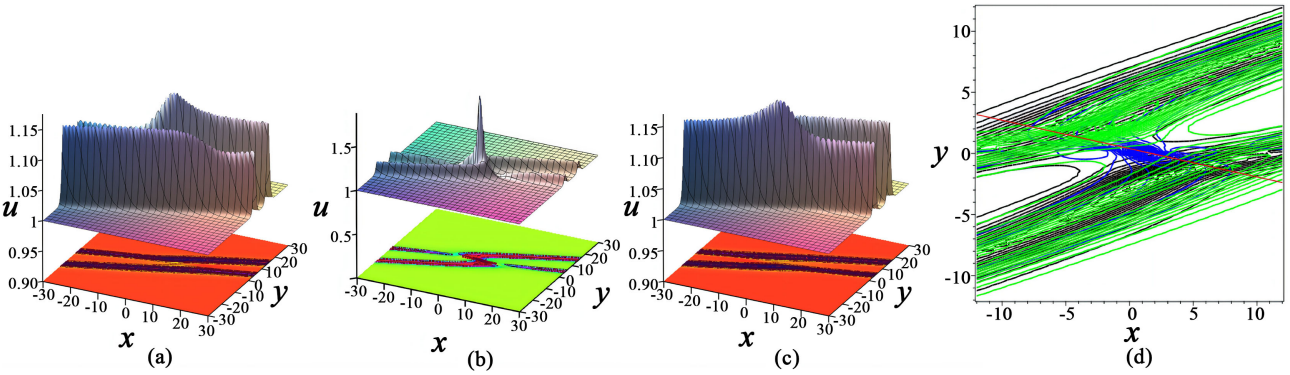

Figure 5. The spatial structure of 1-lump-N-soliton solution at $N = 2$: (a) $t = 30$; (b) $t = 0$; (c) $t = -30$; (d) The trajectory of the lump $y = -\frac{41}{177}x + \frac{70}{177}$ (red), when $t = 30$ (green), 0 (blue), −30 (black).

4. Conclusion

Based on bilinear (3) of Equation (1), we successfully obtained some new lump solutions from breather wave solutions by using parametric limit method, and simulated the evolution and degradation behavior of different forms of breather wave solutions. **Figure 1** and **Figure 2** show the spatial structure evolution of breather characteristic solution degenerated into lump solution. From the form of lump solution, the test function of positive quadratic function superposition is used to get the mixed solution of the equation, and the spatial structure evolution **Figure 3** of lump and soliton with the change of time is given to analyze the

trajectory equation of lump. In Section 3, the theory and inference of lump solution and N soliton superposition are obtained and proved. At the same time, two examples are given and the spatial structure evolution diagram is drawn, the motion trajectory and collision change of lump were given respectively. Moreover, the high-order solutions of various exact solutions and the mutual evolution between the solutions help us better understand and analyze the dynamic behavior of the system. These solutions are of great significance to the theoretical research and application of nonlinear partial differential equations. We have done some rich evolutionary behaviors for the HSI equation, and we hope to study other behaviors in the next work.

Conflicts of Interest

The authors declare no conflicts of interest regarding the publication of this paper.

References

[1] Hirota, R. (2004) The Direct Method in Soliton Theory. Cambridge University Press.

[2] Hirota, R. and Satsuma, J. (1981) Soliton Solutions of a Coupled Korteweg-De Vries Equation. *Physics Letters A*, **85**, 407-408. https://doi.org/10.1016/0375-9601(81)90423-0

[3] Gu, C.H., Hu, H.S. and Zhou, Z.X. (1999) Darbour Transformation in Soliton Theory and Geometric Applications. Shanghai Science and Technology Press.

[4] Rogers, C. and Schief, W.K. (2002) Bäcklund and Darboux Transformations: Geometry and Modern Applications in Soliton Theory. Cambridge University Press. https://doi.org/10.1017/cbo9780511606359

[5] Luo, X. (2020) Semi-Rational and Periodic Wave Solutions for the (3 + 1)-Dimensional Jimbo-Miwa Equation. *The European Physical Journal Plus*, **135**, Article No. 36. https://doi.org/10.1140/epjp/s13360-019-00008-z

[6] Ohta, Y. and Yang, J. (2012) General High-Order Rogue Waves and Their Dynamics in the Nonlinear Schrödinger Equation. *Proceedings of the Royal Society A*: *Mathematical*, *Physical and Engineering Sciences*, **468**, 1716-1740. https://doi.org/10.1098/rspa.2011.0640

[7] Rao, J., Liu, Y., Qian, C. and He, J. (2017) Rogue Waves and Hybrid Solutions of the Boussinesq Equation. *Zeitschrift für Naturforschung A*, **72**, 307-314. https://doi.org/10.1515/zna-2016-0436

[8] Ma, W. (2015) Lump Solutions to the Kadomtsev-Petviashvili Equation. *Physics Letters A*, **379**, 1975-1978. https://doi.org/10.1016/j.physleta.2015.06.061

[9] Onorato, M., Residori, S., Bortolozzo, U., Montina, A. and Arecchi, F.T. (2013) Rogue Waves and Their Generating Mechanisms in Different Physical Contexts. *Physics Reports*, **528**, 47-89. https://doi.org/10.1016/j.physrep.2013.03.001

[10] Li, L. and Dai, Z. (2017) New Homoclinic Rogue Wave Solution for the Coupled Schrodinger-Boussinesq Equation. *The Journal of Nonlinear Sciences and Applications*, **10**, 2642-2648. https://doi.org/10.22436/jnsa.010.05.30

[11] Tan, W. (2019) Evolution of Breathers and Interaction between High-Order Lump Solutions and N-Solitons ($N \to \infty$) for Breaking Soliton System. *Physics Letters A*, **383**, Article ID: 125907. https://doi.org/10.1016/j.physleta.2019.125907

[12] Chen, W., Wang, Y. and Tian, L. (2023) Lump Solution and Interaction Solutions to the Fourth-Order Extended (2 + 1)-Dimensional Boiti-Leon-Manna-Pempinelli Equation. *Communications in Theoretical Physics*, **75**, Article ID: 105003. https://doi.org/10.1088/1572-9494/acf3d6

[13] Qin, C., Tian, S., Wang, X. and Zhang, T. (2018) On Breather Waves, Rogue Waves and Solitary Waves to a Generalized (2 + 1)-Dimensional Camassa-Holm-Kadomtsev-Petviashvili Equation. *Communications in Nonlinear Science and Numerical Simulation*, **62**, 378-385. https://doi.org/10.1016/j.cnsns.2018.02.040

[14] Hu, H. and Yang, C. (2024) Abundant Interaction Solutions of the Integrable (1 + 1)-Dimensional Coupled KdV System. *Mathematical Methods in the Applied Sciences*, **47**, 7017-7027. https://doi.org/10.1002/mma.9954

[15] Zhou, Y., Manukure, S. and Ma, W. (2019) Lump and Lump-Soliton Solutions to the Hirota-Satsuma-Ito Equation. *Communications in Nonlinear Science and Numerical Simulation*, **68**, 56-62. https://doi.org/10.1016/j.cnsns.2018.07.038

[16] Zhang, Z., Yang, X., Li, W. and Li, B. (2019) Trajectory Equation of a Lump before and after Collision with Line, Lump, and Breather Waves for (2 + 1)-Dimensional Kadomtsev-Petviashvili Equation. *Chinese Physics B*, **28**, Article ID: 110201. https://doi.org/10.1088/1674-1056/ab44a3

[17] Chen, S., Yin, Y. and Lü, X. (2024) Elastic Collision between One Lump Wave and Multiple Stripe Waves of Nonlinear Evolution Equations. *Communications in Nonlinear Science and Numerical Simulation*, **130**, Article ID: 107205. https://doi.org/10.1016/j.cnsns.2023.107205

[18] Hietarinta, J. (1997) Introduction to the Hirota Bilinear Method. In: Kosmann-Schwarzbach, Y., Grammaticos, B. and Tamizhmani, K.M., Eds., *Integrability of Nonlinear Systems*, Springer, 95-103. https://doi.org/10.1007/bfb0113694

[19] Tan, W. (2020) Some New Dynamical Behaviour of Double Breathers and Lump-*n*-Solitons for the Ito Equation. *International Journal of Computer Mathematics*, **98**, 961-974. https://doi.org/10.1080/00207160.2020.1792454

[20] Tan, W., Zhang, W. and Zhang, J. (2020) Evolutionary Behavior of Breathers and Interaction Solutions with m-Solitons for (2 + 1)-Dimensional KdV System. *Applied Mathematics Letters*, **101**, Article ID: 106063. https://doi.org/10.1016/j.aml.2019.106063

[21] Tan, W., Dai, Z., Xie, J. and Qiu, D. (2018) Parameter Limit Method and Its Application in the (4 + 1)-Dimensional Fokas Equation. *Computers & Mathematics with Applications*, **75**, 4214-4220. https://doi.org/10.1016/j.camwa.2018.03.023